



Ideas and perspectives: Sensing energy and matter fluxes in a biota-dominated Patagonian landscape through environmental seismology – introducing the Pumalín Critical Zone Observatory

Christian H. Mohr¹, Michael Dietze^{2,3}, Violeta Tolorza⁴, Erwin Gonzalez⁵, Benjamin Sotomayor⁶, Andres Iroume⁷, Sten Gilfert¹, and Frieder Tautz¹

¹Institute of Environmental Sciences and Geography, University of Potsdam, Potsdam, Germany

²Department of Physical Geography, Georg August University, Göttingen, Germany

³Section 4.6 Geomorphology, GFZ Potsdam, Potsdam, Germany

⁴Universidad de la Frontera, Temuco, Chile

⁵Pumalín Douglas Tompkins National Park, Corporación Nacional Forestal (CONAF), Amarillo, Chile

⁶Dron Aerogeomática SpA, Spatial Data and Analysis in Aysén, Coyhaique, Chile

⁷Instituto de Conservación, Biodiversidad y Territorio, Facultad de Ciencias Forestales y Recursos Naturales, Universidad Austral de Chile, Valdivia, Chile

Correspondence: Christian H. Mohr (cmohr@uni-potsdam.de)

Received: 20 April 2023 – Discussion started: 24 April 2023

Revised: 8 September 2023 – Accepted: 8 January 2024 – Published: 28 March 2024

Abstract. The coastal temperate rainforests (CTRs) of Chilean Patagonia are a valuable forest biome on Earth given their prominent role in biogeochemical cycling and the ecological value and dynamics of surface processes. The Patagonian CTRs are amongst the most carbon-rich biomes on Earth. Together with frequent landscape disturbances, these forests potentially allow for episodic and massive release or sequestration of carbon into and from the atmosphere. We argue that, despite their particular biogeographic, geochemical, and ecological roles, the Patagonian CTRs in particular and the global CTRs in general are not adequately represented in the current catalog listing critical zone observatories (CZO). Here, we present the Pumalín CZO as the first of its kind, located in Pumalín National Park in northern Chilean Patagonia. We consider our CZO a representative end-member of undisturbed ecosystem functioning of the Patagonian CTRs. We have identified four core research themes for the Pumalín CZO around which our activities circle in an integrative, quantitative, and generic approach using a range of emerging techniques. Our methodological blend includes an environmental seismology that also fills a critical spatiotemporal scale in terms of monitoring critical zone and surface processes with a minimum interven-

tion in those pristine forests. We aim to gain quantitative understanding of these topics: (1) carbon sink functioning; (2) biota-driven landscape evolution; (3) water, biogeological, and energy fluxes; and (4) disturbance regime understanding. Our findings highlight the multitude of active functions that trees in particular and forests in general may have on the entire cascade of surface processes and the concomitant carbon cycling. This highlights the importance of an integrated approach, i.e., “one physical system”, as proposed by Richter and Billings (2015), and accounts for the recent advances in pushing nature conservation along the Chilean coast.

1 Introduction

Intact forests play a vital role in maintaining Earth's ecosystems because they promote biodiversity (Clark and McLachlan, 2003), accumulate carbon from the atmosphere in exchange for oxygen (thus building important carbon sinks) (Canadell and Raupach, 2008), and regulate global hydrologic and carbon cycles (Bonan, 2008). Forests also modulate geomorphic processes (e.g., Sidle, 1992) and thus landscape

and carbon turnover rates (Hilton et al., 2011; Giesbrecht et al., 2022; Bidlack et al., 2021). In the long run, the biomass (and carbon) of a forest is balanced by growth and mortality rates (e.g., Urrutia-Jalabert et al., 2015; Pan et al., 2011). Tree mortality, the percentage of trees in a population that die in a given year, is also an ecological key metric for species composition and stand density (Searle et al., 2022). In particular, high tree mortality can be triggered by disturbances, such as wind storms, landslides, fire, drought, or pests (e.g., Attiwill, 1994).

Living and dead trees form integral parts of Earth's critical zone (Brantley et al., 2017b). Building on the ecosystem concept (Richter and Billings, 2015), a critical zone (CZ) is defined as a "life-supporting, superficial planetary system extending from the near-surface atmospheric layers that exchange energy, water, particles, and gases with the vegetation and ground layers down through the soil to the deepest bedrock weathering fronts" (Brantley et al., 2017a). In 2005, the Earth science community launched the Critical Zone Exploration Network to promote interdisciplinary research with the help of critical zone observatories (CZO). CZOs are sites aimed at measuring the fluxes of solutes, water, energy, gas, and sediments in a CZ (e.g., Richter et al., 2018; Brantley et al., 2017a). We consider that including surface processes in CZ research is mandatory as these processes may control the quantities, modes, timings, and pathways of matter fluxes (e.g., Rasigraf and Wagner, 2022).

As of the writing of this article, there is no predefined protocol for what a CZO should look like. Thus, there is a wide array of structural and operational CZO concepts based on specific hypothesis testing, topographic and/or climatic gradients (among other gradients), or experimental catchments (e.g., Gaillardet et al., 2018). We are aware of a total of 252 listed CZOs (<http://www.czen.org/content/international-czo-working-group>, last access: 13 October 2022, Fig. 1a). Based on this catalog, we recognize, however, the need to diversify and expand the targeted environments. We argue that, in particular, coastal temperate rainforests (CTRs) are not adequately represented in this catalog, despite their particular biogeochemical, geomorphic, and ecological roles. CTRs provide globally relevant ecological and biogeochemical functions. First, they may store > 1200 MgC ha in biomass (Fig. 1c) forming the world's densest C forest biomes. They accumulate ~ 3 % of the global biomass carbon despite accounting for only 0.3 % of the total forest area (e.g., Keith et al., 2009). The former number is easily doubled when adding subsurface carbon contained in soils and roots (e.g., McNicol et al., 2018; Mohr et al., 2017). Second, high freshwater yields, as reported from the Pacific Northwest, may potentially connect the huge terrestrial carbon reservoirs to marine sinks efficiently (e.g., Bidlack et al., 2021; Giesbrecht et al., 2022). The fjords fringing these forests bury carbon at rates far above the global average, sustaining not only globally important carbon sink functions (Cui et al., 2016; Smith et al., 2015), but also high

and vulnerable marine biodiversity (Fernandez and Castilla, 2005). Third, such efficient carbon burial rates coincide with high landscape turnover rates (e.g., Hilton et al., 2011) due to frequent landscape disturbances scraping the hillslopes. The bulk of the carbon is released in pulses by surface processes mostly triggered by disturbance events. These events initialize the steep and short terrestrial carbon conveyor belts towards the sea (e.g., West et al., 2011; Wang et al., 2016; Frith et al., 2018; Mohr et al., 2017; Korup et al., 2019). However, capturing those infrequent carbon pulses is challenging, and missing them may introduce uncertainties or even bias into carbon budget exercises. For example, estimates of large wood mobility – a relevant quantity within the carbon cycle (e.g., Swanson et al., 2021) – mostly rely on time series composed of single snapshots (e.g., Tontonoz et al., 2017; Sanhueza et al., 2019).

To the best of our knowledge, the Héén Latinee, Hakai, and Maybeso CZOs (or experimental forests) (Jain, 2015) are the only CZOs located within the coastal temperate rainforest biome. Both of these sites lie within the Pacific Northwest (PNW) of North America, and there is currently no comparable site in its Southern Hemisphere counterpart, except for the Institute of Ecological Research Chiloé. This research institute, however, focuses exclusively on ecological research and does not include (eco)geomorphic research (Rozzi et al., 2000). We regard this lack as an important structural and geographical gap that we start filling here with our recently established Pumalín CZO.

2 Pumalín CZO – scope and instrumentation

To enhance our general understanding of disturbance, surface processes, and concomitant carbon flux feedbacks in Patagonian CTRs, we have identified four core research themes for the Pumalín CZO (Fig. 2) and an integrative, generic approach using a range of techniques (see Sect. 3) to gain a quantitative understanding of these topics: (1) carbon sink functioning; (2) biota-driven landscape evolution; (3) water, biogeochemical, and energy fluxes; and (4) disturbance regime understanding. We exemplify our concept using a rainstorm event (see Sect. 2.2, Understanding biota-driven landscape evolution).

Situated in the heart of the Patagonian coastal rainforest biome (Patagonian CTR, Fig. 1b), Pumalín Douglas Tompkins National Park (from here on abbreviated as Pumalín NP) stands out through its role as a site of large-scale philanthropic–environmental conservation efforts (Beer, 2022) that has been receiving international attention for more than 20 years now (Heinrich, 2000). Within the boundaries of the Pumalín NP, the Pumalín CZO comprises a small (16.3 km²) and steep (36.6 ± 16.8°) headwater catchment – Caleta Gonzalo (CG) Catchment (Fig. 1d). Despite covering only a small fraction of the Pumalín NP, we argue that this particular headwater catchment is representa-

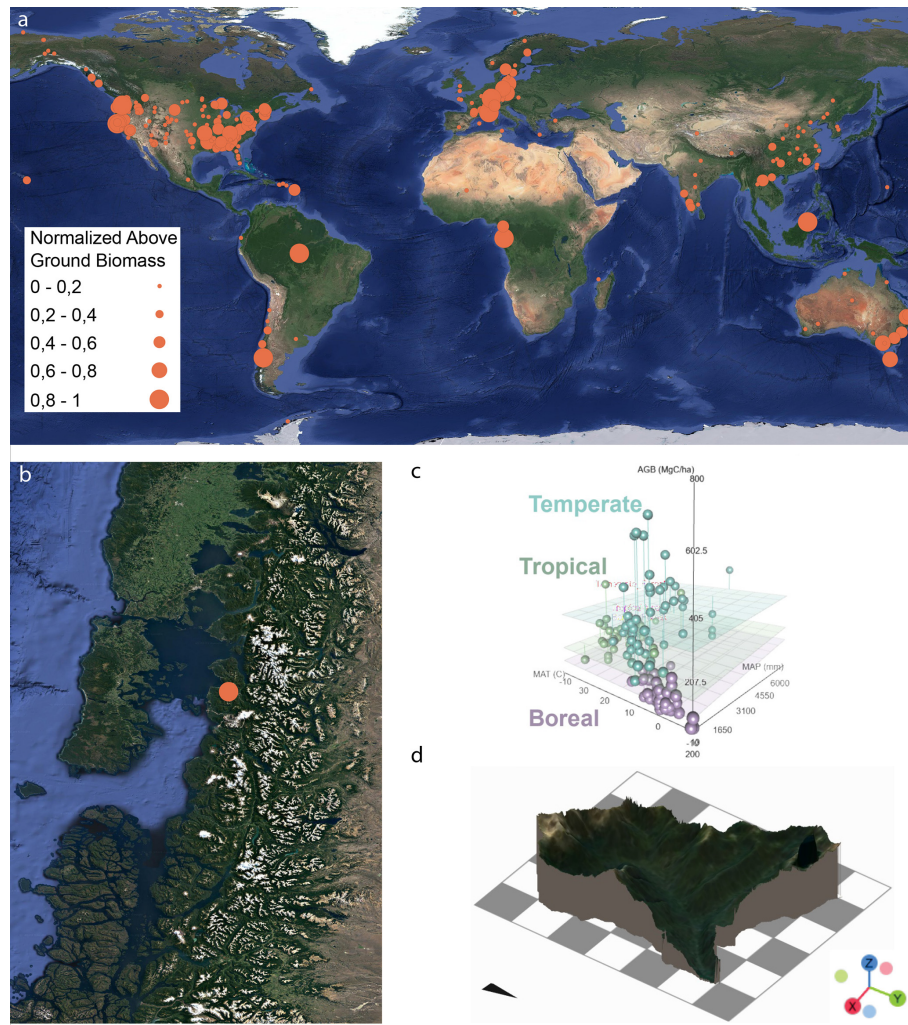


Figure 1. (a) Global distribution of CZOs; the bubble size is scaled to the normalized biomass (<http://www.czen.org/content/international-czo-working-group>, last access: 13 October 2022). Satellite imagery taken from Google Earth (© Google Earth 2015). (b) The Pumalín CZO within the Patagonian rainforest biome (© Google Earth 2015). (c) Estimates of global above-ground biomass C (MgC/ha) as a function of mean annual temperature (°C) (MAT) and precipitation (mm) (MAP) (Keith et al., 2009). (d) 2.5-D visualization of Caleta Gonzalo Catchment as part of the Pumalín CZO, combining airborne lidar-derived DTM and Google Satellite imagery (© Google Earth 2015). No vertical exaggeration: the grid is 1 km × 1 km.

tive of the specific forest biome for several reasons. First, landslide and wind exposure modeling across the entire region does not indicate an exceptional landslide susceptibility or wind exposure status for the CG site (Spors et al., 2022), though there are notably steep gradients in both metrics. As we follow the disturbance exposure sampling design and steep gradients are desirable, CG provides prime preconditions for our research (Fig. 10b). Second, CG is a pristine catchment that hosts some of the largest (and potentially oldest) forest stands within the entire Pumalín NP, shows a typically characteristic forest structure and species composition (e.g., Swanson et al., 2013), and is largely undisturbed by large-scale landscape disturbances, such as earthquake and volcanic-eruption-driven landsliding (Korup et

al., 2019). Therefore, we consider CG an excellent representative end-member of undisturbed ecosystem functioning within the Valdivia ecoregion that hosts the Patagonian CTRs. Between 36 and 47° S, the Patagonian CTR covers some 127 000 km² (DellaSala, 2011). In general, the Patagonian CTR has a cool, wet maritime climate characterized by high precipitation and moderate temperatures (average precipitation \approx 3000–3200 mm yr⁻¹, average temperature \approx 8°C; Alvarez-Garreton et al., 2018; Tecklin et al., 2011) classified as hyperhumid, which supports dense, continuous evergreen broadleaf forests. However, local differences can be high (Alvarez-Garreton et al., 2018). The most common tree species are coihue (*Nothofagus nitida*), mañío (*Podocarpus nubigenus*), canelo (*Drimys winteri*), melí (*Amomyr-*

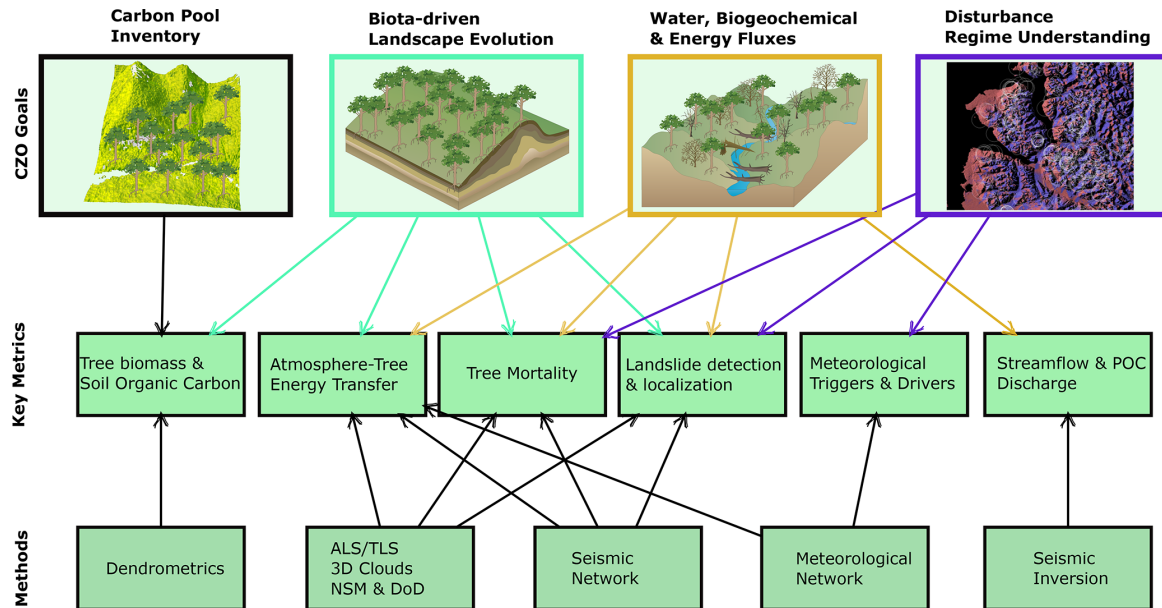


Figure 2. Schematic representation of the four core goals of the Pumalín CZO with the respective key metrics and applied methods. ALS and TLS refer to airborne and terrestrial laser scanning, respectively. DoD and NSM refer to the DEMs of the difference and normalized surface models, respectively.

tus meli), tepa (*Laureliopsis philippiana*), luma (*Amomyrtus luma*), ulmo (*Eucryphia cordifolia*), and arrayan (*Luma apiculata*) (Tecklin et al., 2011; La Barrera et al., 2011; Mohr et al., 2017). Based on plot-scale measurements, estimates of above-ground biomass floodplain forests (42.90° S, 72.69° W, close to Chaitén) are around 370 ± 45 –40 MgC ha, a value that can easily be doubled when including the soils (Mohr et al., 2017). Urrutia-Jalabert et al. (2015) report slightly higher carbon stocks of above-ground biomass (448–517 MgC ha) but old-growth forests at Alerce Andino National Park that are structurally more comparable to the Pumalín forest. The forests are underlain by Pleistocene volcanic sediments covering mostly basement granitoids (Piña-Gauthier et al., 2013). The predominant, carbon-rich soils are 1–2 m deep Andosols (Mohr et al., 2017) setting a maximum bound for shallow landslide thickness. The Chaitén and Michinmahuida volcanoes dominate the park’s topography, which is largely a function of tectonics and glacial erosion leaving behind a spectacular landscape with deep fjords between eroded islands and peninsulas as well as steep slopes and small cirques hosting headwaters above broad, flat-bottomed valleys (Singer et al., 2004). The steep headwater catchments likely facilitate organic carbon export, very much like the topographically similar headwater catchments along the coasts of the Pacific Northwest (Giesbrecht et al., 2022).

The local disturbance regime is comparably simple (Sommerfeld et al., 2018). Widespread insect or pest mortality and fire are much less important than in drier forests. Instead, the dominant forest disturbance comes from frequent

windstorms (Parra et al., 2021) as well as less frequent earthquakes (Sepulveda et al., 2010) and volcanic eruptions (Mohr et al., 2017) – the latter are both a result of active subduction and intra-arc strike–slip motion along the Liquiñe-Ofqui Fault zone (Cembrano et al., 1996). All these disturbances have in common that they may result in mostly shallow landsliding (Korup et al., 2019; Morales et al., 2021). As landslides are largely, though not entirely, controlled by topography and are thus less dependent on vegetation composition (Veblen and Alaback, 1996; DellaSala, 2011; Buma and Johnson, 2015; Parra et al., 2021), we assume them to be largely constrained (and predictable) by topography, which in turn allows us to explore the efficacy of disturbance-driven surface processes on carbon cycling without too many assumptions that are often hard to justify.

2.1 Carbon sink functioning

Our work will contribute to the understanding of broader and general ecological and ecogeomorphic processes in this specific biome, where surface processes along the “carbon cascade” are particularly important (e.g., Booth et al., 2023; Vascik et al., 2021). Only sparse and spatially limited plot-scale-based data on biomass and carbon stocks from the Alerce Andino NP, Chiloe, and the vicinity of Chaitén exist (Urrutia-Jalabert et al., 2015; Mohr et al., 2017). Global biomass products, such as GlobBiomass (Santoro, 2018), GEDI (Duncanson et al., 2022), or regional data (Perez-Quezada et al., 2023), notoriously underestimate these biomass stocks estimated at the plot scale by at least a factor of 2. At the Pumalín

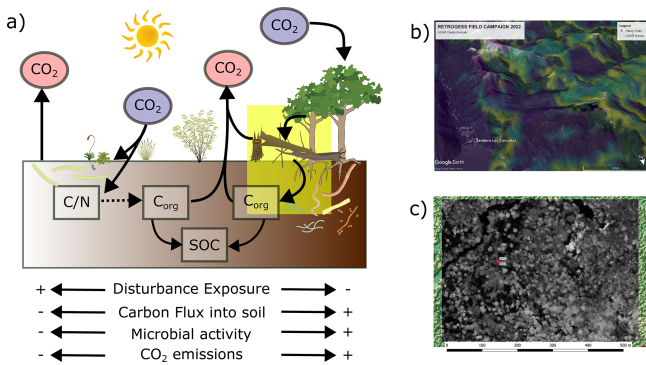


Figure 3. Simplified carbon cycle at the Pumalín CZO. (a) Ignoring CH₄, the main route of carbon into the soil is via autotrophic C fixation by pioneer microbial communities on recent landslide scars, and the diagnostic C/N ratios indicate a qualitative shift on older landslides where carbon fixation is mostly of photosynthetic origin by bacteria and mycorrhizae communities. The yellow box highlights the wind-throw-induced tree mortality (see also Sect. 2.3.1, Tree mortality by wind throw) linking above- and below-ground C pools. (b) Modeled wind exposure for Caleta Gonzalo Catchment following Buma und Johnson (2015) overlaying data from © Google Earth. (c) Lidar-based tree identification using the TREE-TOP algorithm (Silva et al., 2022).

CZO, we link airborne lidar with plot-scale monitoring to deliver the first regional-scale estimate of biomass and carbon stocks, a prerequisite for subsequent carbon flux studies (see Sect. 2.3, Unraveling biogeochemical and energy cycles).

Based on a total of 421 212 detected individual trees within Caleta Gonzalo Catchment (Fig. 3c), our lidar data yield an average density of 258 trees per hectare that, regarding the tree heights, translate into ~ 200 MgC ha when applying species-specific height–DBH relationships (Drake et al., 2003). Our first estimates lie within the range < 120 and 520 MgC ha for the Alerce Andino NP (Urrutia-Jalabert et al., 2015). Our results therefore stress the notion of the Patagonian CTRs as a particularly biomass-rich forest biome on Earth that additionally experiences high surface dynamics activity. However, we anticipate a higher carbon density, given that our ongoing field surveys suggest an underestimation of the total tree number within our lidar data.

In this context, we particularly study at the Pumalín CZO whether, how, and when landslides and wind throw are active geomorphic agents (see Sect. 2.2, Understanding biota-driven landscape evolution) linking both the above- and below-ground carbon pools (Rasigraf and Wagner, 2022) (Fig. 3a, b). Both these processes may bury biomass and soils, thus relocating carbon into the subsurface and/or mixing mineral and organic soil horizons (Kramer et al., 2004). The cascade of tree mortality and/or landsliding, i.e., C input into soils, together with the long-term fate of deadwood and buried carbon in terms of decomposition (C subsurface storage) and transport along the fluvial drainage system (C output), will evolve into one main scientific thread at the

Pumalín CZO. Such cascade knowledge is unconstrained for the entire Patagonian CTR. As the carbon turnover is relatively slow, carbon may be stored as deadwood over centuries in Patagonian CTRs (Urrutia-Jalabert et al., 2015), thus potentially setting up an important more stable and persistent terrestrial carbon buffer. Together, quantifying the carbon input and output terms is key to establishing a first regional carbon balance. Such a balance is urgently needed to assess whether these forests function as carbon sources or sinks, whether such functioning is constant over time, or whether disturbances may cause a transient or permanent switch between both functions – a prerequisite for developing nature-based solutions in terms of climate change. In particular, quantifying the effects of disturbances is pressing, as disturbances are predicted to change in this biome, not only quantitatively, but also qualitatively. The disturbance regime has likely already started to change (e.g., Buma et al., 2019). Both our current capabilities to study such effects and our knowledge of process responses to disturbances are limited and/or ambiguous. For example, state-of-the-art soil organic carbon decomposition models fail under time-varying temperature and moisture regimes (e.g., Wang et al., 2015). Hence, we are not able to predict physically sound and thus transfer long-term effects of disturbed and thus changing boundary conditions on soil organic carbon sequestration. Also, nutrients and vegetation cover progressively accumulate on landslide scars over time, thus increasing the net input of (fixed) carbon into the soil. At the same time, however, such carbon input stimulates microbial life, which in turn accelerates carbon turnover, and the quantitative relevance of such opposing effects is unknown (e.g., Rasigraf and Wagner, 2022; Fig. 3a). Burial of organic-rich sediments beneath landslide deposits further contributes to long-term carbon sequestration (Frith et al., 2018). At the same time, however, forest disturbances can offset the effect of forest carbon sink functioning, e.g., by elevating tree mortality (Seidl et al., 2014b). Hence, we argue that the impact of disturbance on the carbon balance remains highly ambiguous, with erratic, exemplary, and non-systematic and non-quantified evidence for both source and sink functioning. Our Pumalín CZO may help to elucidate such ambiguity in a particularly biomass-rich forest using a “disturbance–exposure” approach (see Sect. 3).

2.2 Understanding biota-driven landscape evolution

Landslide susceptibility coincides with wind exposure along the coasts of southeastern Alaska (Buma and Johnson, 2015) and Patagonia (Fig. 4a). For the latter, a relationship between landslide occurrence, forest cover, and wind speed exists (Parra et al., 2021). This finding is physically meaningful. Tree canopies form wind sails (e.g., Hale et al., 2015), thus transferring momentum from the atmosphere into the shallow subsurface. Aside from wind speed, exposure, and direction (Langre, 2008), the transfer depends on tree phys-

iogonomic metrics, such as the tree drag coefficient, which can vary within a canopy (Jackson et al., 2021). We assume that kinetic energy is transferred from the canopy to the soil through tree swaying inducing ground motion (Fig. 4c, d), and the conversion of kinetic energy to heat is negligible. Ground shaking induced by earthquakes may trigger mass wasting (e.g., Dadson et al., 2004). However, the role of wind-borne ground shaking as a potential trigger for mass wasting is vastly understudied but anecdotal. One of the most important caveats in this context is that previous attempts could not always rule out hidden effects of concomitant rainfall during wind storms (e.g., Rulli et al., 2007; Zhuang et al., 2023). The Pumalín CZO is a particularly suitable location for studying direct, physically based effects of wind on landsliding mechanics because of the presence of strong westerly winds that are channeled by the fjords and occasional strong winds from local ice fields or foehn winds, as reported by Schneider et al. (2014) and Coronato (1993). The locations of both the seismic sensors in Caleta Gonzalo Catchment (Fig. 1d and see also Sect. 3.1, Environmental seismology at the Pumalín CZO) and the meteorological station have mostly northern exposure, and we regard both sites as similar at first order, though we acknowledge that this assumption may be simplified.

Figure 4c–e depict the wind forcing during the exemplary rainstorm on 22 March 2022 (Fig. 5). During that storm, our meteorological station recorded minute-averaged wind speeds of $> 11 \text{ m s}^{-1}$ primarily coming from the west. During the same storm, the Nueva Chaitén station (DMC station no. 420015, -42.78528 , -72.83500), some 30 km southwest of Caleta Gonzalo, registered gusts of $> 20 \text{ m s}^{-1}$, mostly from WNW. The trees responded to wind forcing, as recorded by the tree-mounted seismometer (see Sect. 3.1, Environmental seismology at the Pumalín CZO), in distinct frequency bands of the horizontal components (Fig. 3c) centered at 0.4, 0.95, 2.0, 3.5, 32, and 70 Hz, reaching a maximum spectral power of -64 dB ($10 \log_{10} (\text{m s}^{-1})^2 \text{ Hz}$) at 0.4 Hz and a peak ground velocity (PGV) of $1.42 \times 10^{-2} \text{ m s}^{-1}$ during that storm. The seismic stations in the soils, located some 2 m away from the trees, recorded PGVs of $3.63 \times 10^{-5} \text{ m s}^{-1}$. Following the Wang (2007) empirical though physically derived relationships for earthquake shaking (see also Sect. 3.1), our seismic data may help in quantitatively constraining the transfer of kinetic energy from the atmosphere into the subsurface. We note that our single tree-mounted estimates should however be likely treated as conservative values for mainly three reasons. First, the lidar data only capture the crown canopies of the highest trees but neglect lower-level tree canopies (see height data), which likely results in a considerably higher tree density. Previous studies have shown tree densities of 800 trees per hectare for largely similar conditions (Mohr et al., 2017; Urrutia-Jalabert et al., 2015). Second, the estimated energy density ignores the patchy forest structure. We therefore expect locally higher ground motion and energy densities due to wind forcing

for more exposed and prominent trees. Third, wind speeds $> 20 \text{ m s}^{-1}$ occur in nearby fjords. Data from the Chilean Meteorological Service point to even stronger wind speeds. Thus, we expect higher energy transfer into the ground during stronger winds.

Spors et al. (2022) discovered through physics-based modeling that Patagonian rainforests have the ability to not only recover from cyclical disturbances but also increase stability on hillslopes over time; i.e., disturbances are “healing up” affected landscapes. They also found that an excess of biomass may lead to landslides in Patagonian rainforests, i.e., that forests turn into “suicidal forests”, likely contributing to the overall denudation. In fact, Mohr et al. (2022) found the highest denudation rates along the entire Chilean Andes under dense Patagonian CTRs. This is consistent with previous findings by Vorpahl et al. (2012) for regions where the biomass exceeds 800 Mg ha^{-1} . With its high biomass loads, steep topography, water excess, and multiple disturbances, the Pumalín CZO offers a rare chance to grasp biotic-influenced landscapes over different timescales. Ongoing research indicates that CTR-dominated landscapes operate as a continuum involving soil production, vegetation, physical erosion, and ecohydrological processes (e.g., Mohr et al., 2022). Such a holistic denudational continuum differs from the commonly held assumption that vegetation mainly stabilizes hillslopes, resulting in steep slopes but curbing landsliding.

2.3 Unraveling biogeochemical and energy cycles

Surface processes mobilize, store, and export carbon. Thus, surface processes form an integral part of the Pumalín CZO. At the Pumalín CZO, we (currently) focus on the following three main processes.

2.3.1 Tree mortality by wind throw

Quantifying tree mortality rates is difficult and is approximated using either remote sensing techniques (e.g., He et al., 2019), event-based mapping (e.g., Uriarte et al., 2019), or plot-scale experiments (e.g., Lutz and Halpern, 2006; Urrutia-Jalabert et al., 2015). All these methods have their individual advantages and limitations, yet they introduce drawbacks in terms of spatial and/or temporal resolution and coverage.

As of the writing this paper and in the absence of our own data on tree mortality, we still rely on published tree mortality rates from similar environments. In the Alerce Andino NP (some 100 km to the north), tree mortality links above-ground biomass to the ground pool at rates between < 0.1 and $0.8 \text{ MgC ha yr}^{-1}$ for canelo (*Drimys winteri*) and coihue (*Nothofagus nitida*), respectively (Urrutia-Jalabert et al., 2015). With 277 ± 62 years, the average wood residence times for *Nothofagus nitida*-dominated forests is remarkably high. Leaning on concepts for landslides (Rasigraf and Wag-

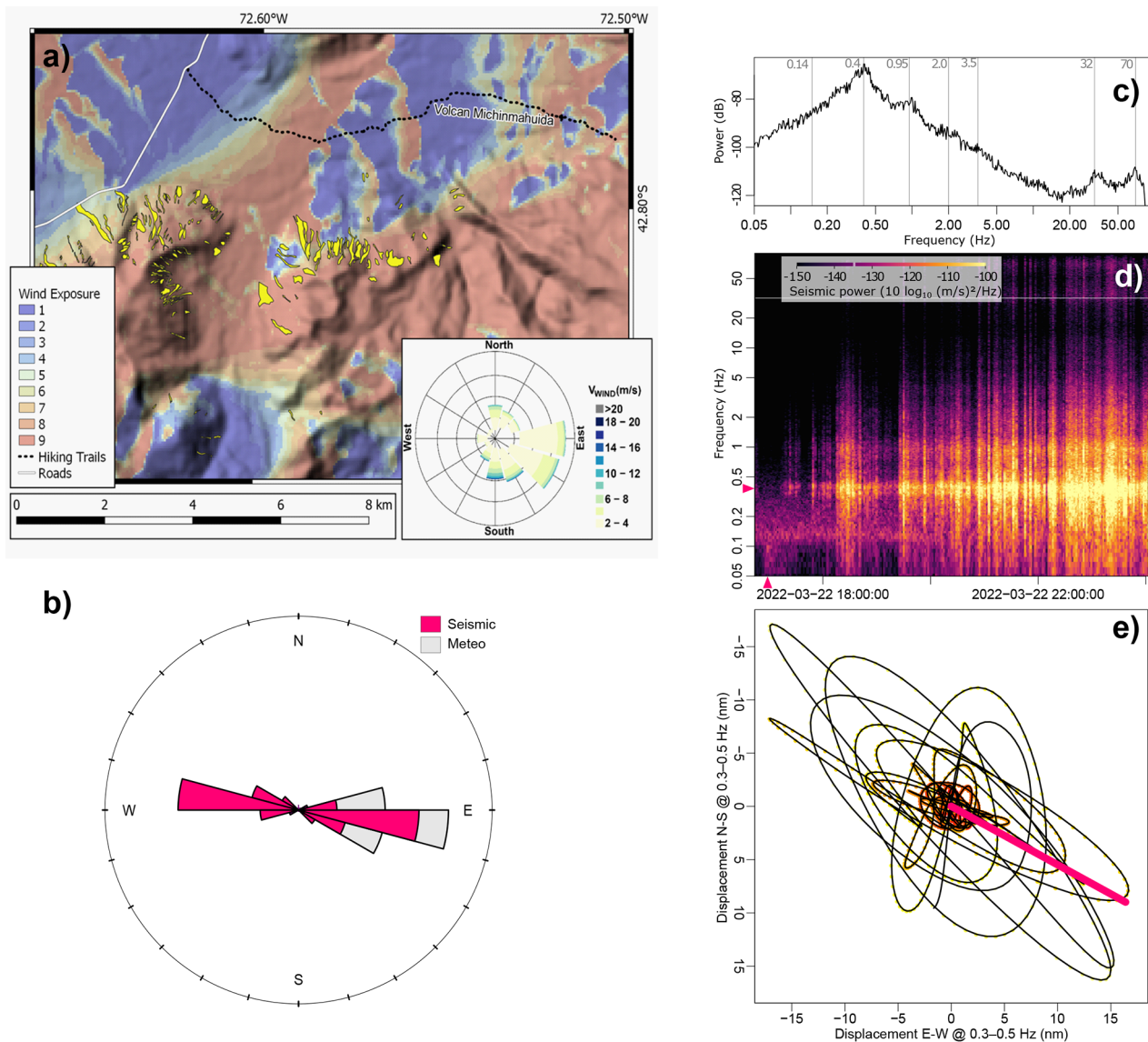


Figure 4. Atmosphere–vegetation energy transfer. **(a)** Modeled wind exposure following Buma and Johnson (2015) using SRTM data overlain by landslide polygons facing north into the Michinmahuida River from the slopes of the Chaitén volcano. **(b)** Rose diagram of both wind direction from the meteorological station and seismically derived tree movement directions. **(c)** Seismic power spectrum averaging over the entire time period of meteorologic forcing during a storm event (CGC04). Grey bars indicate frequencies with local power maxima, except for the 0.15 Hz bar that illustrates the supposed locations of ocean microseisms. **(d)** Seismic power spectrum resolving the temporal evolution of seismic energy during the storm event. Note: wind-speed-invariant ocean microseism frequency band drowning in a storm signal after 20:00 UTC. The pink triangles depict a 1 min time window and a 0.3–0.6 Hz frequency band used to generate **(e)** the sensor displacement trajectory due to tree-bending motion. The colors indicate a 1 min time span from red to yellow. The pink bar represents the mean angle of displacement.

ner, 2022), we regard wind throw as a similar vehicle to link the C pools above and below the ground. With $> 20 \text{ m s}^{-1}$, reported wind speeds frequently exceed wind speed thresholds to trigger tree fall and uprooting across the larger area of interest. Seidl et al. (2014a) report wind-induced tree mortality occurring for wind speeds as low as $> 10 \text{ m s}^{-1}$ for damaged trees and some 20 m s^{-1} for healthy, mature trees. The work by Urrutia-Jalabert et al. (2015) is an important con-

tribution providing the first *measured* tree mortality rates for the Patagonian CTR under presumably undisturbed conditions, i.e., representing background rates. In most cases, this metric is often *assumed* for modeling studies of the Patagonian CTRs (e.g., Gutiérrez and Huth, 2012). At the Pumalín CZO, we seek to overcome such caveats using environmental seismology. Dietze et al. (2020) showed that environmental seismology may capture individual tree fall at distances

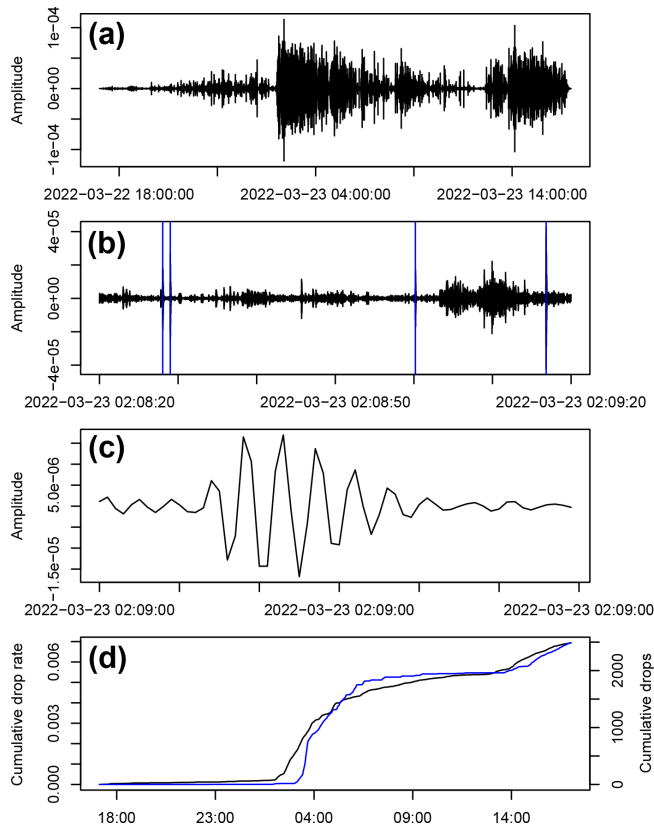


Figure 5. Rain information from seismic sensors. **(a)** The 50–60 Hz filtered seismic waveform of station CGC04 during the period shown in Fig. 9. **(b)** Zoom into a 1 min interval with STA-LTA-picked potential rain drop impacts (blue vertical lines) considering short- and long-term windows of 0.5 and 300 s, respectively, an on ratio of 3, and an off ratio of 1.1. **(c)** Zoom into a single 0.3 s long interval with a 0.15 s long drop impact signal. **(d)** Cumulative seismic (black line) and weather-station-derived (blue line) precipitation record.

as large as 2 km. We therefore anticipate that our CZO will help inform, among others, forest gap models, e.g., Formind (Fischer et al., 2016), to understand ecosystem and carbon dynamics in a more comprehensive way, such as by better implementing forest disturbances in space and time.

2.3.2 Carbon mobilization by landsliding

Our mapped landslides (Fig. 4a) are consistent with the notion of wind effects on landslide occurrence, a finding supported by previous work (Parra et al., 2021). We identified a hillslope event (Fig. 6) that occurred on 22 March 2022 at 03:59:18 UTC and coincided with high rainfall intensity (Fig. 5d). Following the approach by Dietze et al. (2020), we automatically picked potential landslide events. For all the detected events we calculated the spectrograms of all the seismic stations and located the event using the signal migration technique (Burtin et al., 2014) with 5–20 Hz filtered sig-

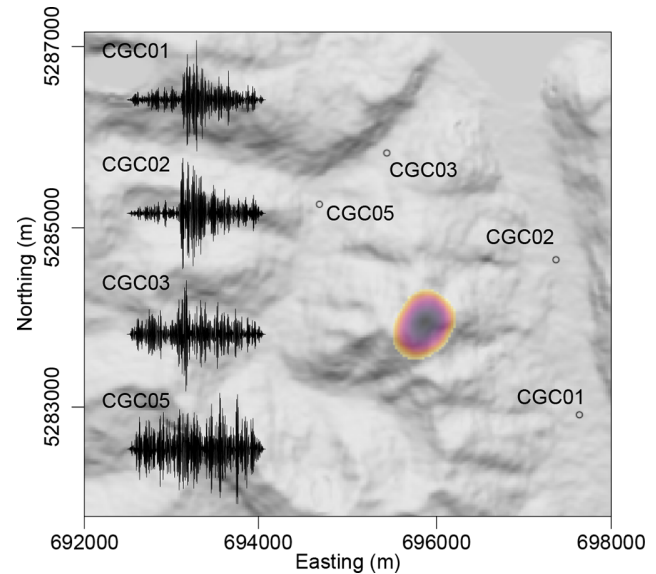


Figure 6. Seismically detected and located hillslope event happening on 22 March 2022 at 03:59:18 UTC. The hillshade map in the background shows Caleta Gonzalo Catchment and the locations of the four ground stations used to locate the event. The colored polygon shows the > 99 % confidence area of the event location. Seismograms (10–15 Hz bandpass-filtered deconvolved waveforms) of 14 s length, with the 7 s event as registered by the four stations. Note that CGC05 close to the waterfall is dominated by the river turbulence signal, in which the mass wasting signature drowns.

nal envelopes, imposing a surface wave propagation velocity of 600 m s^{-1} . That velocity value was found to maximize the overall R^2 value of location estimates across all station combinations. Based on the combined information drawn from the signal waveform, spectrogram, and location, we manually removed unlikely landslide signals following the criteria catalog by Cook and Dietze (2022).

We emphasize that this particular hillslope event occurred under presumably “dry” antecedent conditions as it happened during the transition from austral summer to austral fall (22 March 2022) and that landslide activity is concentrated during the rainy season (Morales et al., 2021). Our CZO may assist in improving rainfall duration–intensity thresholds (Guzzetti et al., 2008), thus providing – together with the wind data – a contribution for early warning, considering known limitations in the spatial variability of storms (Fustos-Toribio et al., 2022). Seismically derived landslide rates may further help shed light on hillslope–channel coupling and, thus, rates of carbon export from hillslopes (Croissant et al., 2021). Intriguingly, suspended sediment concentration (SSC) samples taken in March 2022 point to extraordinarily low SSC concentrations, i.e., $< 0.001 \text{ g L}^{-1}$, even in the immediate aftermath of the rainfall–runoff event, suggesting a high recycling rate of hillslope debris *within* the catchment (a “big compost dump”?) and not necessarily high sediment and organic carbon export into the fjords as noted by Cui

et al. (2016). The resulting landslide scars punch gaps into the forest. These gaps set the stage for high biological diversity induced by a combination of vegetation succession and species that are particularly adapted to disturbance (Walker und Shiels, 2012) and soil microbial life (Rasigraf and Wagner, 2022). As biomass subsequently regrows in the gaps, our CZO may also help decipher direct biomass growth controls on landslide occurrence.

2.3.3 Riverine transport of large wood

Large wood (LW) transport forms an integral part of the regional carbon balance of forested catchments (Swanson et al., 2021). Undoubtedly, post-disturbance LW comprises an important mobile quantity within catchments sustaining Patagonian CTRs (e.g., Ulloa et al., 2015; Mohr et al., 2017; Tonon et al., 2017). However, we are not aware of any quantitative estimate of wood mobility, wood retention, and respective wood residence times under undisturbed conditions within the Patagonian CTRs, and thus the quantification of a background rate of LW mobility is pending. We believe that background rates are required to benchmark single wood pulses as commonly caused or triggered by disturbance. Our CZO starts filling this important knowledge gap by monitoring LW fluxes.

LW mobility nonlinearly but systematically follows flood magnitude (Ruiz-Villanueva et al., 2016). We therefore anticipate predicting LW transport using water stage information and identifying a characteristic frequency band of LW in motion. For our exemplary rainstorm, we estimated a water stage rise from 0.5 to 1.2 m for Caleta Gonzalo Catchment using the Monte Carlo based model inversion approach (Fig. 7). Streamflow started to rise several minutes after rainfall started supporting our assumed short response times for the catchment. Short response times are common for steep headwater catchments (Wohl, 2010).

Lidar is able to penetrate shallow turbulent water despite water velocity, water surface roughness, turbidity, and properties of the river bed negatively affecting the accuracy (Bailey et al., 2012). We argue that the low-flow conditions during the time of the lidar data acquisition allow us to estimate the river bed topography with high confidence, thus developing channel cross sections (Fig. 10d, e) and subsequently translating the water stage into cross-sectional areas of ~ 1.9 and 11.6 m^2 , respectively. We conservatively estimate a surface flow velocity of 2 m s^{-1} judging from field observations, thus yielding a streamflow discharge between 4 m s^{-1} and a maximum of 23 m s^{-1} . These numbers are realistic for steep mountain headwater rivers of that size (Wohl, 2010). The maximum water stage is only 30–40 cm below the bankfull height (Fig. 10d). Exceeding such a threshold is critical for LW transport, because the largest fraction of LW is mobilized during flood events exceeding this specific threshold (e.g., Iroumé et al., 2015). We expect higher water levels and LW mobility during the rainy season. Hence, the

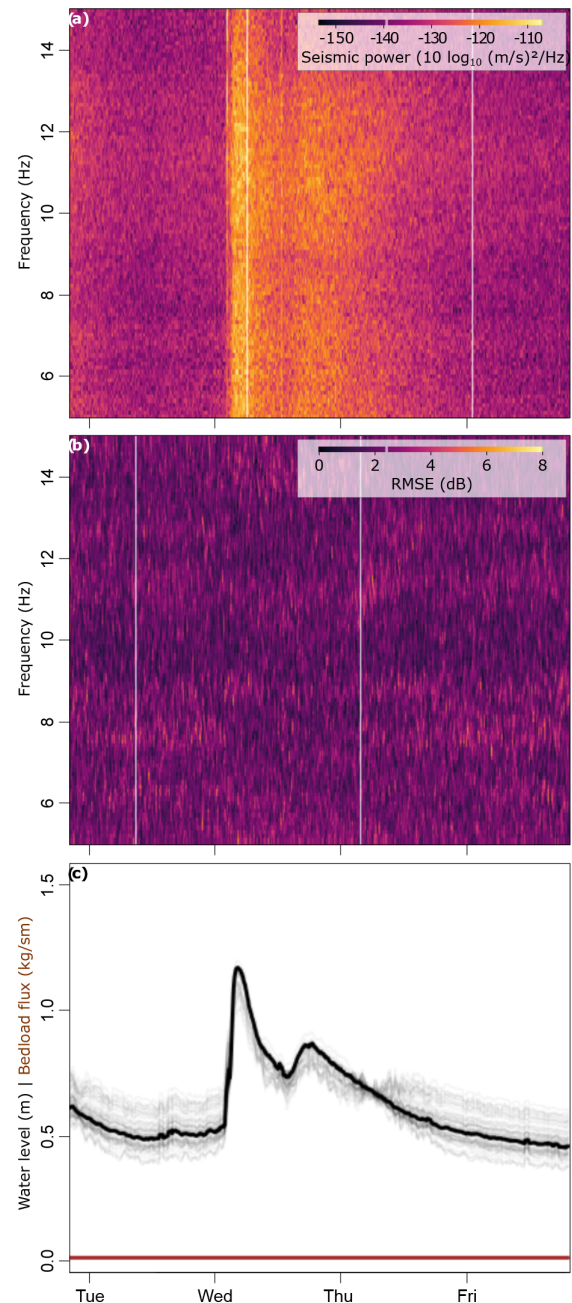


Figure 7. Inversion of seismic power spectra for river dynamics. **(a)** Seismic spectrogram zoomed into the analyzed frequency range 5–15 Hz with a clear broadband power maximum on Wednesday 23 March 2022. **(b)** Root mean square error matrix of modeled and measured spectra. **(c)** Monte Carlo based hydrographs (grey lines) and bedload flux time series (brown lines) for $n = 500$ simulations and five sample window sizes. Thick black and brown lines depict the average results of the former two metrics. Based on UAV imagery, we set river bed particles to range around a D_{50} of 0.2 ± 0.5 (σ) and a channel gradient of 0.05. Consistent with mostly loose cobble and organic-rich material building the river terrace and foot slopes between the river and seismometer, we set the Rayleigh wave velocity to 500 m s^{-1} , the ground quality factor to 23, and the Green function displacement amplitude parameters between 0.6 and 0.8.

Pumalín CZO may provide valuable first benchmark rates for LW mobility in pristine Patagonian CTRs, thus helping to better understand riverine particulate organic carbon (POC) fluxes in this biome.

2.4 Understanding landscape disturbance feedbacks in a holistic ecogeomorphic continuum

Landscape disturbances not only modify the efficacy of erosion, as they may transiently shift systems from a quasi-steady state to higher states (Vanacker et al., 2007), but may also likely cause a (temporal) switch from carbon sink to source functioning (e.g., Mohr et al., 2017). Tectonic disturbances, such as earthquakes (Sepúlveda et al., 2010) and explosive volcanic eruptions (Morales et al., 2021; Korup et al., 2019), are arguably the most powerful yet low-frequency erosion drivers in the Patagonian CTRs. Together with high-frequency wind storms (Parra et al., 2021), these disturbances form the backbone of the regional disturbance regime (Sommerfeld et al., 2018). Disturbances commonly set the scene for ecogeomorphic process cascades (e.g., Gill and Malamud, 2014) that may trigger similar surface processes despite their different driving mechanisms. In the Patagonian CTRs these surface processes comprise abundant, mostly shallow landsliding (Morales et al., 2021) (Fig. 4). However, the *decisive active* role of biota for “disturbance geomorphology” often remains conceptual but rarely quantified. For example, physics-based modeling (Fig. 8) confirms a prime control of gradual loss of shear strength of decaying tree roots in areas of high tephra loads followed by slow subsequent forest regrowth. Together, both opposing trends open a time window for the observed widespread, lagged landsliding mostly several years after forest disturbance (Korup et al., 2019) – a concept known from forestry (Sidle, 1992) but largely unexplored for other forest disturbances. Thus, we argue that the geomorphic system of the Patagonian CTRs is clearly modulated, if not dominated, by biotic processes, and leaving them out of calculations may cause bias and/or incomplete conclusions. The Pumalín CZO faces steep gradients of wind- and landslide-disturbance exposure (see Sect. 3, Methods, design, and instrumentation of the Pumalín CZO), thus allowing us to trade space for time to explore the long-term resilience of the forest ecosystem and recovery traits of the ecogeomorphic system following disturbance and its relation to carbon cycling.

CTRs are subject to rapid climate shifts, and among the expected consequences, strong westerly winds are predicted to become stronger (Perren et al., 2020). Also, the disturbance regime may plausibly change, and new disturbance processes, such as snow-loss-driven mortality, droughts, and fire in historically moist and non-fire-exposed areas, are predicted to emerge. Such predictions are already observed in the Pacific CTRs and, given their similarity, are expected to co-occur in the future along the Patagonian CTRs too (Buma et al., 2019). At the same time, anthropogenic pressure in-

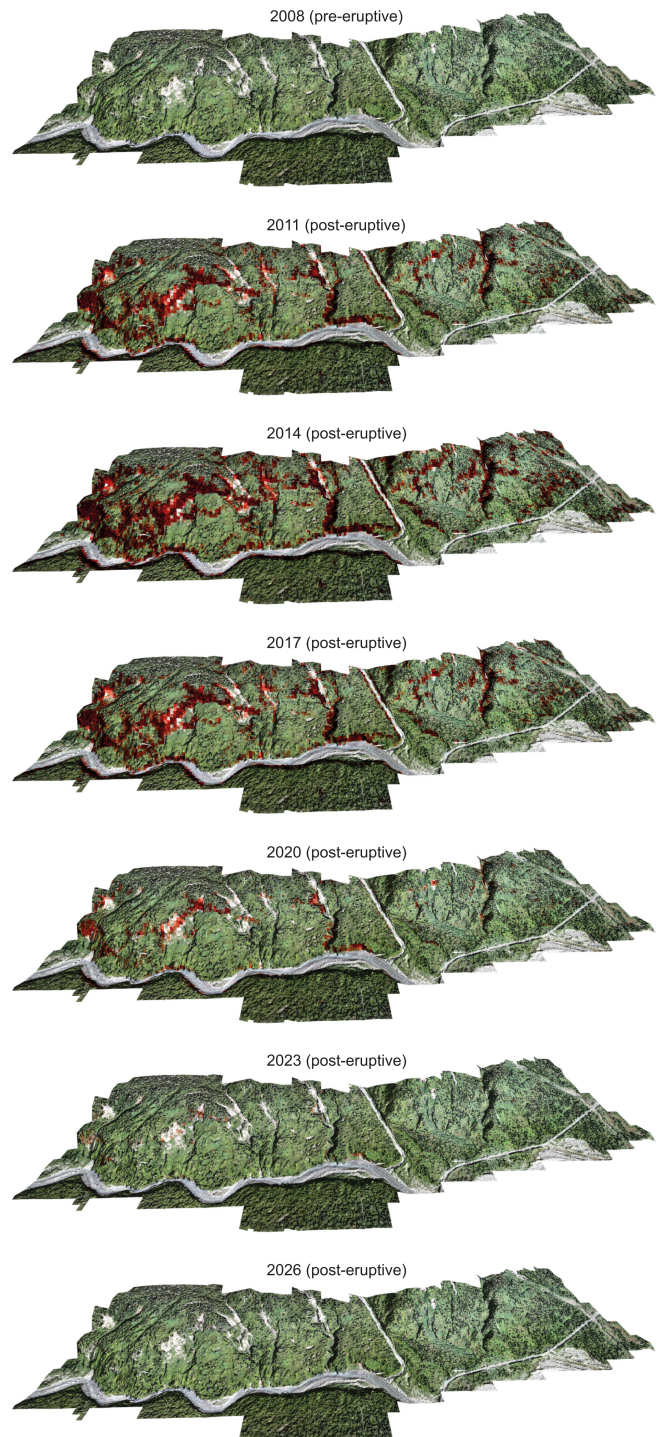


Figure 8. Landlab modeling to predict landslide exposure in red (0–1) along a hillslope of Chaitén volcano disturbed by its 2008 eruption. Landslide exposure has changed over time after the 2008 violent volcanic eruption, which caused root strength decay and subsequent regrowth following the massive forest dieback. Our own UAV-derived post-landslide orthophoto (obtained in March 2018) draped over pre-landslide TanDEM data at a nominal 12.5 m ground resolution.

creases and a southward migration from drier parts of Chile is expected to occur due to climate change (e.g., Balsari et al., 2020). Hence, we need to find solutions to manage in the future a natural system that is constantly changing, presumably at higher rates and magnitudes. Disturbance management is thus increasingly important for sustainable stewardship of forests but also national park managers and requires tools to evaluate the effects of management alternatives on disturbance risk and ecosystem services (Seidl et al., 2014a). We anticipate that our CZO and our approach may assist in that endeavor facilitated by the close collaboration with Corporación Nacional Forestal (CONAF) offices.

3 Methods, design, and instrumentation of the Pumalín CZO

We follow the exposure concept as the backbone for the design of our instrumentation. Exposure is the long-term likelihood of disturbance within a given area, i.e., representing the relative frequency of disturbances within a given area (e.g., Buma and Johnson, 2015). Hence, disturbance exposure gradients are similar to the widely applied concept of chronosequences (e.g., Rasigraf and Wagner, 2022) but substitute time with space. To address the goals and collect the required metrics with a sustainable set of sensors, we combine four different complementary approaches (Fig. 3): (1) periodic field surveys (biomass estimation, landscape scanning) to constrain the landscape architecture; (2) control data records of key variables that drive landscape dynamics (meteorological sensors, soil moisture and temperature, imagery-based stream gauges) at selected representative sites; (3) physics-based, biota-focused geomorphic modeling (Fig. 8); and (4) environmental seismology (Fig. 9). Our seismic approach (see the details in Sect. 3.1, Environmental seismology at the Pumalín CZO) goes beyond the list of goals identified (Fig. 3). More importantly, it is not just about the metrics we can measure with the help of this particular method but how we can simultaneously assess them across both timescales and space scales. Existing sensors are specialized for specific variables, but they have either limited spatial coverage or significant time gaps. For instance, to monitor tree mortality in forests, we use geophones placed in the ground. Previous studies focused on small plot scales (problematic for estimating tree mortality due to its limited spatial scope) or remote sensing. However, remote sensing often lacks fine spatial detail and might miss falling small trees hidden by the canopy. This information is crucial, especially when studying future carbon cascades. Given our methodological blend, we not only study an understudied biome and its ecogeomorphic processes but also address critical spatial gaps. Therefore, the seismic approach nicely complements existing methods bridging technological research gaps. This is particularly relevant for CZOs in remote areas focused on Earth surface processes. Such an in-

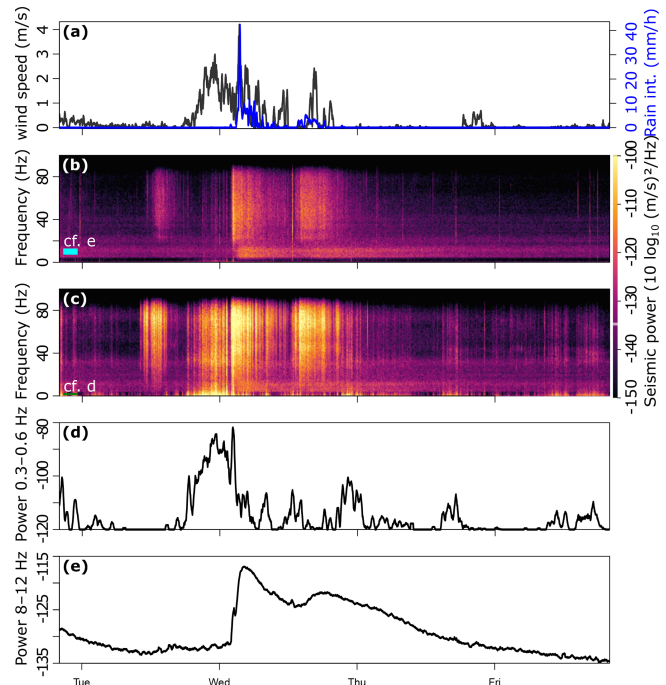


Figure 9. Field measurements of a small rainstorm. (a) Meteorological sensor data on wind-speed and precipitation intensity. (b) Seismic spectrogram of a sensor deployed in the ground (CGC03), showing episodic broadband signals (30–80 Hz) due to meteorologic forcing and a continuous low-frequency signal (8–12 Hz) due to turbulent water flow in a nearby river. (c) Seismic spectrogram of a sensor (CGC04) mounted on a tree, 5 m away, which exhibits considerably more seismic power, predominantly at frequencies < 1 Hz. (d) Average seismic power in the 0.3–0.6 Hz band, representing tree motion in the atmospheric wind field. Values below -120 dB were set to -120 dB. (e) Average seismic power in the 8–12 Hz frequency band, indicative of river discharge.

tegrative approach, along with the representativeness of the CG site, offers a generic and scalable tool set to explore the cascading and/or feedback roles of forests, disturbances, biomass, and concomitant carbon fluxes.

3.1 Environmental seismology at the Pumalín CZO

Environmental seismology is arguably one of the most recent advances in studying critical-zone processes (Oakley et al., 2021), most likely for four main reasons. This technique allows continuous and weather-independent determination of the (1) location, (2) timing, and (3) magnitude of (near-)surface processes (Dietze et al., 2020) (4) while being minimally invasive at the same time. As of October 2022 we were operating six seismic stations consisting of Digos DataCube digitizers that record with 200 Hz ground motion data from 4.5 Hz geophone sensors, which are either deployed in the ground or mounted to trunks at breast height (Fig. 10b). Our system is able to operate for about 12 months without data extraction and battery replacement maintenance visits,

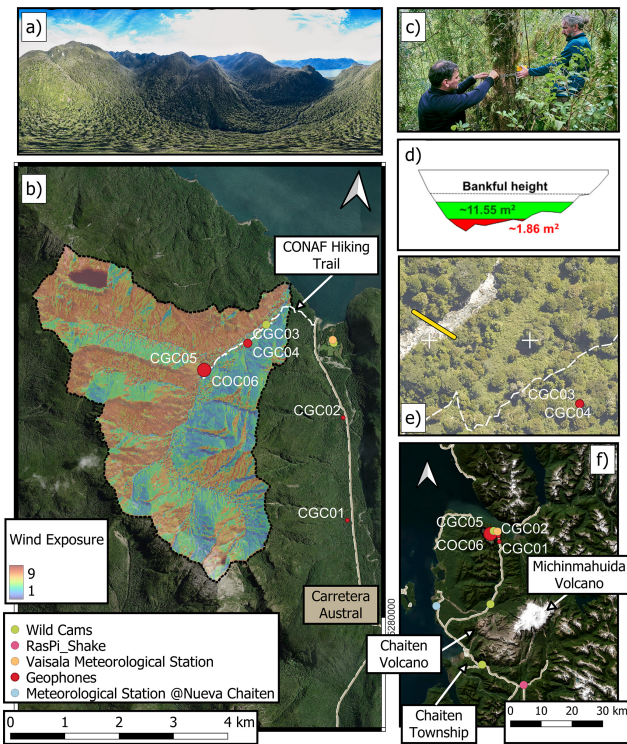


Figure 10. Overview of the Pumalín CZO. (a) A 360° panoramic view of Caleta Gonzalo Catchment acquired using a DJI Phantom 4 pro v2.0 drone during the field campaign in March 2002. (b) Map showing the locations of the instruments deployed within Caleta Gonzalo Catchment and along the Carretera Austral overlain by modeled wind exposure. Bubble size of geophone scales with averaged wind exposure (0–9) around a 30 m buffer. White dashed line indicates the CONAF-operated hiking trail “Escada escondida”. (c) Mounting of a geophone on a tree trunk (CG04) during fieldwork in March 2022. (d) Cross section of the Gonzalo River and the respective cross-sectional area estimates during the example rainfall–runoff event (see Fig. 5) < 70 m from the geophone CG04 (see panel e). Elevation data come from airborne lidar obtained during the low water stage (November 2021). (f) Caleta Gonzalo Catchment embedded in the larger study area or the Pumalín NP. The blue circle depicts the location of the nearest operating meteorological station © Nueva Chaitén. All the satellite imagery is taken from Google Earth (© Google Earth 2015), except for panel (e). All the photos were taken by the authors.

thus providing a monitoring tool for less accessible sites, as is the case here. The ground-deployed sensors are used to infer river characteristics, energy emission from the atmosphere into the ground, and event-based landslide activity that can be located by the seismic network as a whole.

Rivers also generate seismic waves due to force fluctuations at the river bed caused by eddies in turbulent flow (Gimbert et al., 2014) and mobile particles impacting the river bed (Tsai et al., 2012). Those two river-borne signals cover a source–receiver-specific yet different frequency range and can thus be unmixed by inverse modeling (Dietze et al.,

2019) to yield physically meaningful time series of water level and bedload transport. Here, we follow the inversion approach by Dietze et al. (2022) using seismic data from station GC03, which is located about 70 m from the 12 m wide reach of the river draining CG Catchment (Fig. 10e) to calculate the compound median curves for water stage and bedload fluxes (Fig. 7).

3.2 Forest biomass and carbon stocks at the Pumalín CZO

The currently available tree biomass, setting the pool of carbon that can be released by surface processes, e.g., mass wasting, and subsequently transported to marine carbon sinks, will be estimated by a blend of field-based measurements of tree diameter at breast height (DBH) and the respective heights of representative plots, following a matrix of wind and landslide disturbance gradients and remote sensing. We use our pairwise measurements of DBH and respective tree height to develop empirical relationships between both metrics. We next apply this function to the airborne lidar-based tree heights to predict the spatially resolved DBH. Using both metrics, we can then estimate above-ground biomass by applying species-specific allometric functions for Chilean forests (Drake et al., 2003). We use the relative abundance of tree species to weigh an averaged biomass load using an MC approach (Mohr et al., 2017). In addition, periodic airborne laser scanning (ALS) data sets will support the update of that pool for the entire region of interest.

3.3 Meteorological station at the Pumalín CZO

In March 2022 we deployed a first meteorological station close to the airfield at Caleta Gonzalo (−42.56213868, −72.60038295). Our Vaisala WXT530 meteorological station deployed on a pole 2 m above the ground records air temperature, pressure, relative moisture, wind speed and direction, as well as precipitation type, intensity, and amount at a temporal resolution of 1 min. The Vaisala station is connected to a Campbell CR1000 logger that also stores the soil moisture at 20 cm depth at a temporal resolution of 10 min. For the sake of simplicity and given a largely though not entirely comparable landscape architecture (e.g., a valley opening to the north) and the close proximity, we consider this information to be comparable to local conditions in Caleta Gonzalo Catchment at first order. The DMC station at Nueva Chaitén provides independent meteorological data against which to compare our field-based measurements.

4 Conclusions and perspectives

Having highlighted the multiple active functions that trees and forests may have on energy and matter fluxes, calls for an integrative approach, i.e., “one physical system” as proposed by Richter and Billings (2015), and accounting for the recent

advances in pushing nature conservation along the Chilean Patagonian coast, we advocate for the Pumalín CZO embedded in the spectacular Patagonian CTRs as an ideal addition to the joint, transdisciplinary efforts of exploring the critical zone. In this spirit, we regard the Pumalín CZO, which fully meets the requirements of a CZO, as a valuable member of the international CZO network. To the best of our knowledge, the Pumalín CZO is the first of its kind in the Patagonian CTRs.

The Pumalín NP CZO is expected to expand, including the Michinmahuida Catchment at ~25 km south of Caleta Gonzalo Catchment. This second catchment is also fed by the Michinmahuida glacier, thus adding a second hydrological regime that is characteristic of the Patagonian headwaters, is particularly sensitive to changes in the global climate, and was severely disturbed by the violent 2008 Chaitén eruption (VEI 4, e.g., Lara 2009).

Having presented the four different core goals of the Pumalín CZO (Fig. 3), we anticipate that integrative modeling suites, such as Landlab (Barnhart et al., 2020; Hobbey et al., 2017) that is also informed by scale-bridging environmental seismology, will be excellent and promising tools for placing our findings from such a low-access site into a transferable and thus scalable context (Fig. 8). Developing respective process components will be one prime effort for future research.

Lastly, we want to invite the community to joint efforts in doing critical zone research in this spot on Earth.

Code availability. All the R and Python codes are available upon request from the corresponding author before they are made available for download from a repository.

Data availability. All the data are available upon request from the corresponding author before they are made available for download from a GFZ-hosted repository.

Author contributions. CHM set up the monitoring design with input from MD and VT and acquired funding. Sensor deployment was carried out by CHM, MD, VT, BS, SG, and FT. Data analysis and modeling were carried out by CHM and MD. AI and EG provided local ground support and access to the wonderful sites within the Pumalín NP and helped with logistics and maintenance. CHM wrote the manuscript with the help of all the co-authors.

Competing interests. The contact author has declared that none of the authors has any competing interests.

Disclaimer. Publisher's note: Copernicus Publications remains neutral with regard to jurisdictional claims made in the text, published maps, institutional affiliations, or any other geographical rep-

resentation in this paper. While Copernicus Publications makes every effort to include appropriate place names, the final responsibility lies with the authors.

Acknowledgements. Christian H. Mohr, Sten Gilfert, and Frieder Tautz acknowledge funding provided by DFG grant no. 493703771. Violeta Tolorza received funding from postdoctoral grant VRIP20P001, FONDECYT 11190864, and DFG grant no. 493703771. Andres Iroume acknowledges funding provided by FONDECYT 1200079. We thank the entire CONAF crew of the Pumalín NP as well as the Rewilding Chile Foundation, formerly known as Tompkins Conservation Chile, for conserving this marvelous forest, for permitting our research, and for providing access to our study sites. We cordially thank Torsten Queisser for the best technical support one can imagine. We thank the associate editor, Susan Brantley, and an anonymous reviewer for the constructive reviews.

Financial support. This research has been supported by the Deutsche Forschungsgemeinschaft (grant no. 493703771), ANID/FONDECYT (grant nos. 1200079 and 11190864), and the Universidad de La Frontera (postdoc grant VRIP20P001).

Review statement. This paper was edited by Christopher Still and reviewed by Susan Brantley and one anonymous referee.

References

- Alvarez-Garreton, C., Mendoza, P. A., Boisier, J. P., Addor, N., Galleguillos, M., Zambrano-Bigiarini, M., Lara, A., Puelma, C., Cortes, G., Garreaud, R., McPhee, J., and Ayala, A.: The CAMELS-CL dataset: catchment attributes and meteorology for large sample studies – Chile dataset, *Hydrol. Earth Syst. Sci.*, 22, 5817–5846, <https://doi.org/10.5194/hess-22-5817-2018>, 2018.
- Attiwill, P. M.: The Disturbance of Forest Ecosystems – the Ecological Basis For Conservative Management, *For. Ecol. Manage.*, 63, 247–300, 1994.
- Bailly, J.-S., Kinzel, P. J., Allouis, T., Feurer, D., and Le Coarer, Y.: Airborne LiDAR Methods Applied to Riverin, in: *Fluvial remote sensing for science and management*, edited by: Carbonneau, P. E. and Piégay, H., Bd. 3, Chichester, Wiley-Blackwell (Advancing river restoration and management), ISBN 9780470714270, 2012.
- Balsari, S., Dresser, C., and Leaning, J.: Climate Change, Migration, and Civil Strife, *Curr. Env. Health Rep.*, 7, 404–414, <https://doi.org/10.1007/s40572-020-00291-4>, 2020.
- Barnhart, K. R., Hutton, E. W. H., Tucker, G. E., Gasparini, N. M., Istanbuluoglu, E., Hobbey, D. E. J., Lyons, N. J., Mouchene, M., Nudurupati, S. S., Adams, J. M., and Bandaragoda, C.: Short communication: Landlab v2.0: a software package for Earth surface dynamics, *Earth Surf. Dynam.*, 8, 379–397, <https://doi.org/10.5194/esurf-8-379-2020>, 2020.
- Beer, C. M.: Bankrolling biodiversity: The politics of philanthropic conservation finance in Chile, *Env. Plan. E: Nat. Space*, 6, 1191–1213, <https://doi.org/10.1177/25148486221108171>, 2022.

- Bidlack, A. L., Bisbing, S. M., Buma, B. J., Diefenderfer, H. L., Fellman, J. B., Floyd, W. C., Giesbrecht, I., Lally, A., Lertzman, K. P., Perakis, S. S., Butman, D. E., D'Amore, D. D., Fleming, S. W., Hood, E. W., Hunt, B. P. V., Kiffney, P. M., McNicol, G., Menounos, B., and Tank, S. E.: Climate-Mediated Changes to Linked Terrestrial and Marine Ecosystems across the Northeast Pacific Coastal Temperate Rainforest Margin, *BioSci.*, 71, 581–595, <https://doi.org/10.1093/biosci/biaa171>, 2021.
- Booth, A. M., Buma, B., and Nagorski, S.: Effects of Landslides on Terrestrial Carbon Stocks With a Coupled Geomorphic-Biologic Model: Southeast Alaska, United States, *J. Geophys. Res.-Biogeosci.*, 128, e2022JG007297, <https://doi.org/10.1029/2022JG007297>, 2023.
- Brantley, S. L., Goldhaber, M. B., and Ragnarsdottir, K. V.: Crossing Disciplines and Scales to Understand the Critical Zone, *Elements*, 3, 307–314, <https://doi.org/10.2113/gselements.3.5.307>, 2007.
- Brantley, S. L., McDowell, W. H., Dietrich, W. E., White, T. S., Kumar, P., Anderson, S. P., Chorover, J., Lohse, K. A., Bales, R. C., Richter, D. D., Grant, G., and Gaillardet, J.: Designing a network of critical zone observatories to explore the living skin of the terrestrial Earth, *Earth Surf. Dynam.*, 5, 841–860, <https://doi.org/10.5194/esurf-5-841-2017>, 2017a.
- Brantley, S. L., Eissenstat, D. M., Marshall, J. A., Godsey, S. E., Balogh-Brunstad, Z., Karwan, D. L., Papuga, S. A., Roering, J., Dawson, T. E., Evaristo, J., Chadwick, O., McDonnell, J. J., and Weathers, K. C.: Reviews and syntheses: on the roles trees play in building and plumbing the critical zone, *Biogeosciences*, 14, 5115–5142, <https://doi.org/10.5194/bg-14-5115-2017>, 2017b.
- Buma, B. and Johnson, A. C.: The role of windstorm exposure and yellow cedar decline on landslide susceptibility in southeast Alaskan temperate rainforests, *Geomorphology*, 228, 504–511, <https://doi.org/10.1016/j.geomorph.2014.10.014>, 2015.
- Buma, B., Battlori, E., Bisbing, S., Holz, A., Saunders, S., L. Bidlack, A., Creutzburg, M. K., DellaSala, D. A., Gregovich, D., Hennon, P., Krapek, J., Moritz, M. A., and Zaret, K.: Emergent freeze and fire disturbance dynamics in temperate rainforests, *Austral. Ecol.*, 44, 812–826, <https://doi.org/10.1111/aec.12751>, 2019.
- Clark, J. S. and McLachlan, J. S.: Stability of forest biodiversity, *Nature*, 423, 635–638, <https://doi.org/10.1038/nature01632>, 2003.
- Cook, K. L. and Dietze, M.: Seismic Advances in Process Geomorphology, *Ann. Rev. Earth Planet. Sci.*, 50, 183–204, <https://doi.org/10.1146/annurev-earth-032320-085133>, 2022.
- Coronato, F. R.: Wind chill factor applied to Patagonian climatology, *Int. J. Biometeorol.*, 37, 1–6, <https://doi.org/10.1007/bf01212759>, 1993.
- Croissant, T., Hilton, R. G., Li, G. K., Howarth, J., Wang, J., Harvey, E. L., Steer, P., and Densmore, A. L.: Pulsed carbon export from mountains by earthquake-triggered landslides explored in a reduced-complexity model, *Earth Surf. Dynam.*, 9, 823–844, <https://doi.org/10.5194/esurf-9-823-2021>, 2021.
- Cui, X., Bianchi, T. S., Savage, C., and Smith, R. W.: Organic carbon burial in fjords: Terrestrial versus marine inputs, *Earth Planet. Sc. Lett.*, 451, 41–50, <https://doi.org/10.1016/j.epsl.2016.07.003>, 2016.
- Dadson, S. J., Hovius, N., Chen, H., Dade, W. B., Lin, J. C., Hsu, M. L., Lin, C.-W., Horng, M.-J., Chen, T.-C., Milliman, J., and Stark, C.-P.: Earthquake-triggered increase in sediment delivery from an active mountain belt, *Geology*, 32, 733–736, 2004.
- de Langre, E.: Effects of Wind on Plants, *Ann. Rev. Fluid Mech.*, 40, 141–168, <https://doi.org/10.1146/annurev.fluid.40.111406.102135>, 2008.
- DellaSala, D. A.: Temperate and Boreal Rainforests of the World: Ecology and Conservation, Washington, DC, Island Press/Center for Resource Economics, <https://doi.org/10.5822/978-1-61091-008-8>, 2011.
- Dietze, M., Lagarde, S., Halfi, E., Laronne, J. B., and Turowski, J. M.: Joint sensing of bedload flux and water depth by seismic data inversion, *Water Resour. Res.*, 55, 9892–9904, <https://doi.org/10.1029/2019WR026072>, 2019.
- Dietze, M., Cook, K. L., Illien, L., Rach, O., Puffpaff, S., Stodan, I., and Hovius, N.: Impact of Nested Moisture Cycles on Coastal Chalk Cliff Failure Revealed by Multiseasonal Seismic and Topographic Surveys, *J. Geophys. Res.-Earth*, 125, 1–17, <https://doi.org/10.1029/2019JF005487>, 2020.
- Dietze, M., Hoffmann, T., Bell, R., Schrott, L., and Hovius, N.: A seismic approach to flood detection and characterization in upland catchments, *Geophys. Res. Lett.*, 49, e2022GL100170, <https://doi.org/10.1029/2022GL100170>, 2022.
- Drake, F., Emanuelli, P., and Acuña, E.: Compendio de funciones dendrométricas del bosque nativo, Santiago de Chile, CONAF GTZ, <https://bibliotecadigital.ciren.cl/items/9e2c4ff0-c14a-414c-a6fd-fe73295eda8b> (last access: 26 March 2024), 2003.
- Duncanson, L., Kellner J., Armston, J., Dubayah, R., Minor, D., Hancock, S., Healey, S., Patterson, P., Saarela, S., Marselis, S., Silva, C., Bruening, J., Goetz, S., Tang, H., Hofton, M., Blair, B., Luthcke, S., Fatoyinbo, L., Abernethy, K., Alonso, A., Andersen, H.-E., Aplin, P., Baker, T., Barbier, N., Bastin, J., Biber, P., Boeckx, P., Bogaert, J., Boschetti, L., Brehm Boucher, P., Boyd, D., Burslem, D., Calvo-Rodriguez, S., Chave, J., Chazdon, R., Clark, D., Clark, D., Cohen, W., Coomes, D., Corona, P., Cushman, P., Cutler, M., Dalling, J., Dalponte, M., Dash, J., de-Miguel, S., Deng, S., Woods Ellis, P., Erasmus, B., Fekety, P., Fernandez-Landa, A., Ferraz, A., Fischer, R., Fisher, A., García-Abril, A., Gobakken, T., Hacker, J., Heurich, M., Hill, R., Hopkinson, C., Huang, H., Hubbell, S., Hudak, A., Huth, A., Imbach, B., Jeffery, K., Katoh, M., Kearsley, E., Kenfack, D., Kljun, N., Knapp, N., Král, K., Krůček, M., Labrière, N., Lewis, S., Longo, M., Lucas, R., Main, R., Manzanera, J., Vázquez Martínez, R., Mathieu, R., Memiaghe, H., Meyer, V., Mendoza, A., Moneris, A., Montesano, P., Morsdorf, F., Næsset, E., Naidoo, L., Nilus, R. O'Brien, M., Orwig, D., Papathanassiou, K., Parker, G., Philipson, C., Phillips, O., Pisek, J., Poulsen, J., Pretzsch, H., Rüdiger, C., Saatchi, S., Sanchez-Azofeifa, A., Sanchez-Lopez, N., Scholes, R., Silva, C., Simard, S., Skidmore, A., Stereńczak, K., Tanase, M., Torresan, C., Valbuena, R., Verbeeck, H., Vrska, T., Wessels, K., White, J., White, L., Zahabu, E., and Zraggen, C.: Aboveground biomass density models for NASA's Global Ecosystem Dynamics Investigation (GEDI) lidar mission, *Remote Sens. Environ.*, 270, 112845, <https://doi.org/10.1016/j.rse.2021.112845>, 2022.
- Fernandez, M. and Castilla, J. C.: Marine Conservation in Chile: Historical Perspective, Lessons, and Challenges, *Cons. Biol.*, 19, 1752–1762, <https://doi.org/10.1111/j.1523-1739.2005.00277.x>, 2005.

- Fischer, R., Bohn, F., Dantas de Paula, M., Dislich, C., Groenewald, J., Gutiérrez, A. G., Kazmierczak, M., Knapp, N., Lehmann, S., Paulick, S., Pütz, S., Rödig, E., Taubert, F., Köhler, P., and Huth, A.: Lessons learned from applying a forest gap model to understand ecosystem and carbon dynamics of complex tropical forests, *Ecol. Model.*, 326, 124–133, <https://doi.org/10.1016/j.ecolmodel.2015.11.018>, 2016.
- Frith, N. V., Hilton, R. G., Howarth, J. D., Gröcke, D. R., Fitzsimons, S. J., Croissant, T., Wang, J., McClymont, E. L., Dahl, J., and Densmore, A. L.: Carbon export from mountain forests enhanced by earthquake-triggered landslides over millennia, *Nat. Geosci.*, 11, 772–776, <https://doi.org/10.1038/s41561-018-0216-3>, 2018.
- Fustos-Toribio, I., Manque-Roa, N., Vásquez Antipan, D., Hermosilla Sotomayor, M., and Letelier Gonzalez, V.: Rainfall-induced landslide early warning system based on corrected mesoscale numerical models: an application for the southern Andes, *Nat. Hazards Earth Syst. Sci.*, 22, 2169–2183, <https://doi.org/10.5194/nhess-22-2169-2022>, 2022.
- Gaillardet, J., Braud, I., Hankard, F., Anquetin, S., Bour, O., Dorflinger, N., de Dreuzy, J. R., Galle, S., Galy, C., Gogo, S., Gourcy, L., Habets, F., Laggoun, F., Longuevergne, L., Le Borgne, T., Naaim-Bouvet, F., Nord, G., Simonneaux, V., Six, D., Tallec, T., Valentin, C., Abril, G., Allemand, P., Arènes, A., Arfib, B., Arnaud, L., Arnaud, N., Arnaud, P., Audry, S., Comte, V. B., Batiot, C., Batais, A., Bellot, H., Bernard, E., Bertrand, C., Bessière, H., Binet, S., Bodin, J., Bodin, X., Boithias, L., Bouchez, J., Boudevillain, B., Moussa, I. B., Branger, F., Braun, J. J., Brunet, P., Caceres, B., Calmels, D., Cappelaere, B., Celle-Jeanton, H., Chabaux, F., Chalikhakis, K., Champollion, C., Copard, Y., Cotel, C., Davy, P., Deline, P., Delrieu, G., Demarty, J., Dessert, C., Dumont, M., Emblanch, C., Ezzahar, J., Estèves, M., Favier, V., Faucheux, M., Filizola, N., Flammarion, P., Floury, P., Fovet, O., Fournier, M., Francez, A. J., Gandois, L., Gascuel, C., Gayer, E., Genthon, C., Gérard, M. F., Gilbert, D., Gouttevin, I., Grippa, M., Gruau, G., Jardani, A., Jeanneau, L., Join, J. L., Jourde, H., Karbou, F., Labat, D., Lagadeuc, Y., Lajeunesse, E., Lasnet, R., Lavado, W., Lawin, E., Lebel, T., Le Bouteiller, C., Legout, C., Lejeune, Y., Le Meur, E., Le Moigne, N., Lions, J., Lucas, A., Malet, J. P., Marais-Sicre, C., Maréchal, J. C., Marlin, C., Martin, P., Martins, J., Martinez, J. M., Massei, N., Mauclerc, A., Mazzilli, N., Molénat, J., Moreira-Turcq, P., Mougin, E., Morin, S., Ngoupayou, J. N., Panthou, G., Peugeot, C., Picard, G., Pierret, M. C., Porel, G., Probst, A., Probst, J. L., Rabatel, A., Raclot, D., Ravanel, L., Rejiba, F., René, P., Ribolzi, O., Riotte, J., Rivière, A., Robain, H., Ruiz, L., Sanchez-Perez, J. M., Santini, W., Sauvage, S., Schoeneich, P., Seidel, J. L., Sekhar, M., Sengtaeuanghoung, O., Silvera, N., Steinmann, M., Soruco, A., Tallec, G., Thibert, E., Lao, D. V., Vincent, C., Viville, D., Wagnon, P., and Zitouna, R.: OZCAR: The French Network of Critical Zone Observatories, *Vadose Z. J.*, 17, 180067, <https://doi.org/10.2136/vzj2018.04.0067>, 2018.
- Giesbrecht, I. J. W., Tank, S. E., Frazer, G. W., Hood, E., Gonzalez A., Santiago G., Butman, D. E., D'Amore, D. V., Hutchinson, D., Bidlack, A., and Lertzman, K. P.: Watershed Classification Predicts Streamflow Regime and Organic Carbon Dynamics in the Northeast Pacific Coastal Temperate Rainforest, *Global Biogeochem. Cy.*, 36, e2021GB007047, <https://doi.org/10.1029/2021GB007047>, 2022.
- Gill, J. C. and Malamud, B. D.: Reviewing and visualizing the interactions of natural hazards, *Rev. Geophys.*, 52, 680–722, <https://doi.org/10.1002/2013RG000445>, 2014.
- Gutiérrez, A. G. and Huth, A.: Successional stages of primary temperate rainforests of Chiloé Island, Chile. *Persp. Plant Ecol., Evol. Syst.*, 14, 243–256, <https://doi.org/10.1016/j.ppees.2012.01.004>, 2012.
- Guzzetti, F., Peruccacci, S., Rossi, M., and Stark, C. P.: The rainfall intensity–duration control of shallow landslides and debris flows: an update, *Landslides*, 5, 3–17, <https://doi.org/10.1007/s10346-007-0112-1>, 2018.
- Hale, S. E., Gardiner, B., Peace, A., Nicoll, B., Taylor, P., and Pizzirani, S.: Comparison and validation of three versions of a forest wind risk model, *Environ. Modell. Softw.*, 68, 27–41, <https://doi.org/10.1016/j.envsoft.2015.01.016>, 2015.
- He, Y., Chen, G., Potter, C., and Meentemeyer, R. K.: Integrating multi-sensor remote sensing and species distribution modeling to map the spread of emerging forest disease and tree mortality, *Remote Sens. Environ.*, 231, 111238, <https://doi.org/10.1016/j.rse.2019.111238>, 2019.
- Heinrich, P.: Visiting a Very Large Paradise, *The New York Times*, <https://www.nytimes.com/2000/01/30/travel/visiting-a-very-large-paradise.html> (last access: 25 March 2024), 2000.
- Hilton, R. G., Meunier, P., Hovius, N., Bellingham, P. J., and Galy, A.: Landslide impact on organic carbon cycling in a temperate montane forest, *Earth Surf. Proc. Land.*, 36, 1670–1679, 2011.
- Hobley, D. E. J., Adams, J. M., Nudurupati, S. S., Hutton, E. W. H., Gasparini, N. M., Istanbuloglu, E., and Tucker, G. E.: Creative computing with Landlab: an open-source toolkit for building, coupling, and exploring two-dimensional numerical models of Earth-surface dynamics, *Earth Surf. Dynam.*, 5, 21–46, <https://doi.org/10.5194/esurf-5-21-2017>, 2017.
- Iroumé, A., Mao, L., Andreoli, A., Ulloa, H., and Ardiles, M. P.: Large wood mobility processes in low-order Chilean river channels, *Geomorphology*, 228, 681–693, <https://doi.org/10.1016/j.geomorph.2014.10.025>, 2015.
- Jackson, T. D., Sethi, S., Dellwik, E., Angelou, N., Bunce, A., van Emmerik, T., Duperat, M., Ruel, J.-C., Wellpott, A., Van Bloem, S., Achim, A., Kane, B., Ciruzzi, D. M., Loheide II, S. P., James, K., Burcham, D., Moore, J., Schindler, D., Kolbe, S., Wiegmann, K., Rudnicki, M., Lieffers, V. J., Selker, J., Gougherty, A. V., Newson, T., Koeser, A., Miesbauer, J., Samelson, R., Wagner, J., Ambrose, A. R., Detter, A., Rust, S., Coomes, D., and Gardiner, B.: The motion of trees in the wind: a data synthesis, *Biogeosciences*, 18, 4059–4072, <https://doi.org/10.5194/bg-18-4059-2021>, 2021.
- Jain, T. B.: Northwest research experimental forests: A hundred years in the making, *West. Forest.*, 60, 1–4, 2015.
- Keith, H., Mackey, B. G., and Lindenmayer, D. B.: Re-evaluation of forest biomass carbon stocks and lessons from the world's most carbon-dense forests, *P. Natl. Acad. Sci. USA*, 106, 11635–11640, <https://doi.org/10.1073/pnas.0901970106>, 2009.
- Korup, O., Seidemann, J., and Mohr, C. H.: Increased landslide activity on forested hillslopes following two recent volcanic eruptions in Chile, *Nat. Geosci.*, 12, 284–290, <https://doi.org/10.1038/s41561-019-0315-9>, 2019.

- Kramer, M. G., Sollins, P., and Sletten, R. S.: Soil carbon dynamics across a windthrow disturbance sequence in southeast Alaska, *Ecology*, 85, 2230–2244, <https://doi.org/10.1890/02-4098>, 2004.
- La Barrera, F., de Reyes-Paecke, S., and Meza, L.: Landscape analysis for rapid ecological assessment of relocation alternatives for a devastated city, *Rev. Chil. Hist. Nat.*, 84, 181–194, 2011.
- Lutz, J. A. and Halpern, C. B.: Tree mortality during early forest development: A long-term study of rates, causes, and consequences, *Ecol. Monogr.*, 76, 257–275, [https://doi.org/10.1890/0012-9615\(2006\)076\[0257:TMDEFD\]2.0.CO;2](https://doi.org/10.1890/0012-9615(2006)076[0257:TMDEFD]2.0.CO;2), 2006.
- McNicol, G., Bulmer, C., D'Amore, D., Sanborn, P., Saunders, S., Giesbrecht, I. J. W., Gonzalez-Arriola, S., Bidlack, A., Butman, D., and Buma, B.: Large, climate-sensitive soil carbon stocks mapped with pedology-informed machine learning in the North Pacific coastal temperate rainforest, *Environ. Res. Lett.*, 14, 014004, <https://doi.org/10.1088/1748-9326/aaed52>, 2018.
- Mohr, C. H., Korup, O., Ulloa, H., and Iroumé, A.: Pyroclastic Eruption Boosts Organic Carbon Fluxes Into Patagonian Fjords, *Global Biogeochem. Cy.*, 31, 1626–1638, <https://doi.org/10.1002/2017GB005647>, 2017.
- Mohr, C. H., Tolorza, V., Georgieva, V., Munack, H., Wilcken, K. M., Fülöp, R.-H., Codilean, A., Parra, E., and Carretier, S.: Dense vegetation promotes denudation in Patagonian rainforests, *Earth Space Sci. Open Arch.*, 40, 1–40, <https://doi.org/10.1002/essoar.10511846.1>, 2022.
- Morales, B., Lizama, E., Somos-Valenzuela, M. A., Lillo-Saavedra, M., Chen, N., and Fustos, I.: A comparative machine learning approach to identify landslide triggering factors in northern Chilean Patagonia, *Landslides*, 18, 2767–2784, <https://doi.org/10.1007/s10346-021-01675-9>, 2021.
- Oakley, D. O. S., Forsythe, B., Gu, X., Nyblade, A. A., and Brantley, S. L.: Seismic Ambient Noise Analyses Reveal Changing Temperature and Water Signals to 10 s of Meters Depth in the Critical Zone, *J. Geophys. Res.-Earth*, 126, e2020JF005823, <https://doi.org/10.1029/2020JF005823>, 2021.
- Pan, Y., Birdsey, R. A., Fang, J., Houghton, R., Kauppi, P. E., Kurz, W. A., Phillips, O. L., Shvidenko, A., Lewis, S. L., Canadell, J. G., Ciais, P., Jackson, R. B., Pacala, S. W., McGuire, D., Piao, S., Rautiainen, A., Sitch, S., and Hayes, D.: A Large and Persistent Carbon Sink in the World's Forests, *Science*, 333, 988–993, <https://doi.org/10.1126/science.1201609>, 2011.
- Parra, E., Mohr, C. H., and Korup, O.: Predicting Patagonian Landslides: Roles of Forest Cover and Wind Speed, *Geophys. Res. Lett.*, 48, e2021GL095224, <https://doi.org/10.1029/2021GL095224>, 2021.
- Perez-Quezada, J. F., Moncada, M., Barrales, P., Urrutia-Jalabert, R., Pfeiffer, M., Herrera, A., and Farías, S.: How much carbon is stored in the terrestrial ecosystems of the Chilean Patagonia?, *Austral. Ecol.*, 48, 893–903, <https://doi.org/10.1111/aec.13331>, 2023.
- Perren, B. B., Hodgson, D. A., Roberts, S. J., Sime, L., van Nieuwenhuijze, W., Verleyen, E., and Vyverman, W.: Southward migration of the Southern Hemisphere westerly winds corresponds with warming climate over centennial timescales, *Commun. Earth Environ.*, 1, 1–8, <https://doi.org/10.1038/s43247-020-00059-6>, 2020.
- Rasigraf, O. and Wagner, D.: Landslides: An emerging model for ecosystem and soil chronosequence research, *Earth-Sci. Rev.*, 231, 104064, <https://doi.org/10.1016/j.earscirev.2022.104064>, 2022.
- Richter, D. and Billings, S. A.: “One physical system”: Tansley's ecosystem as Earth's critical zone, *New Phytol.*, 206, 900–912, <https://doi.org/10.1111/nph.13338>, 2015.
- Richter, D. D., Billings, S. A., Groffman, P. M., Kelly, E. F., Lohse, K. A., McDowell, W. H., White, T. S., Anderson, S., Baldocchi, D. D., Banwart, S., Brantley, S., Braun, J. J., Brecheisen, Z. S., Cook, C. W., Hartnett, H. E., Hobbie, S. E., Gaillardet, J., Jobbagy, E., Jungkunst, H. F., Kazanski, C. E., Krishnaswamy, J., Markewitz, D., O'Neill, K., Riebe, C. S., Schroeder, P., Siebe, C., Silver, W. L., Thompson, A., Verhoef, A., and Zhang, G.: Ideas and perspectives: Strengthening the biogeosciences in environmental research networks, *Biogeosciences*, 15, 4815–4832, <https://doi.org/10.5194/bg-15-4815-2018>, 2018.
- Rozzi, R., Silander, J., Armesto, J. J., Feinsinger, P., and Massardo, F.: Three levels of integrating ecology with the conservation of South American temperate forests: the initiative of the Institute of Ecological Research Chiloé, Chile, *Biodiv. Conserv.*, 9, 1199–1217, <https://doi.org/10.1023/A:1008909121715>, 2000.
- Ruiz-Villanueva, V., Wyźga, B., Zawiejska, J., Hajdukiewicz, M., and Stoffel, M.: Factors controlling large-wood transport in a mountain river, *Geomorphology*, 272, 21–31, <https://doi.org/10.1016/j.geomorph.2015.04.004>, 2016.
- Rulli, M. C., Meneguzzo, F., and Rosso, R.: Wind control of storm-triggered shallow landslides, *Geophys. Res. Lett.*, 34, L03402, <https://doi.org/10.1029/2006GL028613>, 2007.
- Sanhueza, D., Picco, L., Ruiz-Villanueva, V., Iroumé, A., Ulloa, H., and Barrientos, G.: Quantification of fluvial wood using UAVs and structure from motion, *Geomorphology*, 345, 106837, <https://doi.org/10.1016/j.geomorph.2019.106837>, 2019.
- Santoro, M.: GlobBiomass – global datasets of forest biomass, PANGAEA [data set], <https://doi.org/10.1594/PANGAEA.894711>, 2018.
- Schneider, W., Pérez-Santos, I., Ross, L., Bravo, L., Seguel, R., and Hernández, F.: On the hydrography of Puyuhuapi Channel, Chilean Patagonia, *Progr. Oceanogr.*, 129, 8–18, <https://doi.org/10.1016/j.pocean.2014.03.007>, 2014.
- Searle, E. B., Chen, H. Y. H., and Paquette, A.: Higher tree diversity is linked to higher tree mortality, *P. Natl. Acad. Sci. USA*, 119, e2013171119, <https://doi.org/10.1073/pnas.2013171119>, 2022.
- Seidl, R., Rammer, W., and Blennow, K.: Simulating wind disturbance impacts on forest landscapes: Tree-level heterogeneity matters, *Environ. Modell. Softw.*, 51, 1–11, <https://doi.org/10.1016/j.envsoft.2013.09.018>, 2014a.
- Seidl, R., Schelhaas, M.-J., Rammer, W., and Verkerk, P. J.: Increasing forest disturbances in Europe and their impact on carbon storage, *Nat. Clim. Change*, 4, 806, <https://doi.org/10.1038/nclimate2318>, 2014b.
- Sepúlveda, S. A., Serey, A., Lara, M., Pavez, A., and Rebolledo, S.: Landslides induced by the April 2007 Aysén Fjord earthquake, Chilean Patagonia, *Landslides*, 7, 483–492, <https://doi.org/10.1007/s10346-010-0203-2>, 2010.
- Sidle, R. C.: A theoretical model of the effects of timber harvesting on slope stability, *Water Resour. Res.*, 28, 1897–1910, <https://doi.org/10.1029/92wr00804>, 1992.
- Silva, C. A., Hudak, A. T., Vierling, L. A., Valbuena, R., Cardil, A., Mohan, M., Alves de Almeida, D. R., Broadbent, E. N., Almeyda Zambrano, A. M., Wilkinson, B., Sharma, A., Drake, J. B., Med-

- ley, P. B., Vogel, J. G., Atticciati Prata, G., Atkins, J. W., Hamamura, C., Johnson, D. J., and Klauberg, C.: treetop: A Shiny-based application and R package for extracting forest information from LiDAR data for ecologists and conservationists, *Methods Ecol. Evol.*, 13, 1164–1176, <https://doi.org/10.1111/2041-210X.13830>, 2022.
- Smith, R. W., Bianchi, T. S., Allison, M., Savage, C., and Galy, V.: High rates of organic carbon burial in fjord sediments globally, *Nat. Geosci.*, 8, 450–453, <https://doi.org/10.1038/ngeo2421>, 2015.
- Sommerfeld, A., Senf, C., Buma, B., D’Amato, A. W., Després, T., Díaz-Hormazábal, I., Fraver, S., Frelich, L. E., Gutiérrez, A. G., Hart, S. J., Harvey, B., J., He, H. S., Hlasny, T., Holz, A., Kitzberger, T., Kulakowski, D., Lindenmayer, D., Mori, A. S., Mueller, J., Paritsis, J., Perry, G. L. W., Stephens, S. L., Svoboda, M., Turner, M. G., and Seidl, R.: Patterns and drivers of recent disturbances across the temperate forest biome, *Nat. Commun.*, 9, 4355, <https://doi.org/10.1038/s41467-018-06788-9>, 2018.
- Spors, S., Istanbuluoglu, E., Tolorza, V., and Mohr, C.: Suicidal forests? – Modelling biomass surcharge as a potential landslide driver in temperate rainforests of Chilean Patagonia, EGU General Assembly 2022, Vienna, Austria, 23–27 May 2022, EGU22-4002, <https://doi.org/10.5194/egusphere-egu22-4002>, 2022.
- Swanson, F. J., Jones, J. A., Crisafulli, C. M., and Lara, A.: Effects of volcanic and hydrologic processes on forest vegetation: Chaitén Volcano, Chile, *Andean Geol.*, 40, 359–391, 2013.
- Swanson, F. J., Gregory, S. V., Iroumé, A., Ruiz-Villanueva, V., and Wohl, E.: Reflections on the history of research on large wood in rivers, *Earth Surf. Proc. Land.*, 46, 55–66, <https://doi.org/10.1002/esp.4814>, 2021.
- Tecklin, D., DellaSalla, D. A., Luebert, F., and Pliscoff, P.: Valdivian Temperate Rainforests of Chile and Argentina, in: *Temperate and Boreal Rainforests of the World: Ecology and Conservation*, edited by: DellaSalla, D. D., Washington, DC, Island Press/Center for Resource Economics, 132–153, https://doi.org/10.5822/978-1-61091-008-8_5, 2011.
- Tonon, A., Iroumé, A., Picco, L., Oss-Cazzador, D., and Lenzi, M. A.: Temporal variations of large wood abundance and mobility in the Blanco River affected by the Chaitén volcanic eruption, southern Chile, *Catena*, 156, 149–160, <https://doi.org/10.1016/j.catena.2017.03.025>, 2017.
- Ulloa, H., Iroumé, A., Picco, L., Korup, O., Lenzi, M. A., Mao, L., and Ravazzolo, D.: Massive biomass flushing despite modest channel response in the Rayas River following the 2008 eruption of Chaitén volcano, Chile, *Geomorphology*, 250, 397–406, <https://doi.org/10.1016/j.geomorph.2015.09.019>, 2015.
- Uriarte, M., Thompson, J., and Zimmerman, J. K.: Hurricane María tripled stem breaks and doubled tree mortality relative to other major storms, *Nat. Commun.*, 10, 1362, <https://doi.org/10.1038/s41467-019-09319-2>, 2019.
- Urrutia-Jalabert, R., Malhi, Y., and Lara, A.: The Oldest, Slowest Rainforests in the World?, Massive Biomass and Slow Carbon Dynamics of *Fitzroya cupressoides* Temperate Forests in Southern Chile, *PLoS One*, 10, e0137569, <https://doi.org/10.1371/journal.pone.0137569>, 2015.
- Vanacker, V., von Blanckenburg, F., Govers, G., Molina, A., Poesen, J., Deckers, J., and Kubik, P.: Restoring dense vegetation can slow mountain erosion to near natural benchmark levels, *Geology*, 35, 303, <https://doi.org/10.1130/G23109A.1>, 2007.
- Vascik, B. A., Booth, A. M., Buma, B., and Berti, M.: Estimated Amounts and Rates of Carbon Mobilized by Landsliding in Old-Growth Temperate Forests of SE Alaska, *J. Geophys. Res.-Biogeo.*, 126, e2021JG006321, <https://doi.org/10.1029/2021JG006321>, 2021.
- Vorpahl, P., Elsenbeer, H., Marker, M., and Schroder, B.: How can statistical models help to determine driving factors of landslides?, *Ecol. Model.*, 239, 27–39, 2012.
- Walker, L. R. and Shiels, A. B.: *Landslide Ecology*, Cambridge University Press (Ecology, Biodiversity and Conservation), Cambridge, <https://doi.org/10.1017/CBO9780511978685>, 2012.
- Wang, C. Y.: Liquefaction beyond the Near Field, *Seismol. Res. Lett.*, 78, 512–517, 2007.
- Wang, J. Z., Hilton, R. G., Zhang, F., Li, G., Densmore, A. L., Gröcke, D. R., Xu, X., and West, A. J.: Earthquake-triggered increase in biospheric carbon export from a mountain belt, *Geology*, 44, 471–474, <https://doi.org/10.1130/g37533.1>, 2016.
- Wang, Z., van Oost, K., and Govers, G.: Predicting the long-term fate of buried organic carbon in colluvial soils, *Global Biogeochem. Cy.*, 29, 65–79, <https://doi.org/10.1002/2014GB004912>, 2015.
- West, A. J., Lin, C. W., Lin, T. C., Hilton, R. G., Liu, S. H., Chang, C. T., Lin, K.-C., Galy, A., Sparkes, R. B., and Hovius, N.: Mobilization and transport of coarse woody debris to the oceans triggered by an extreme tropical storm, *Limnol. Oceanogr.*, 56, 77–85, <https://doi.org/10.4319/lo.2011.56.1.0077>, 2011.
- Wohl, E. E.: Mountain rivers revisited, AGU Water Resources Monograph, 19, American Geophysical Union, <https://doi.org/10.1029/WM019>, 2010.
- Zhuang, Y., Xing, A., Petley, D., Jiang, Y., Sun, Q., Bilal, M., and Yan, J.: Elucidating the impact of trees on landslide initiation throughout a typhoon: Preferential infiltration, wind load and root reinforcement, *Earth Surf. Proc. Land.*, 48, 3128–3141, <https://doi.org/10.1002/esp.5686>, 2023.